

## Improvement of Cycling Performance of $\text{Na}_{2/3}\text{Co}_{2/3}\text{Mn}_{1/3}\text{O}_2$ Cathode by PEDOT/PSS Surface Coating for Na Ion Batteries

Yatim Lailun Ni'mah<sup>1\*</sup>, Ju-Hsiang Cheng<sup>2</sup>, Ming-Yao Cheng<sup>2</sup>, Wei-Nien Su<sup>2</sup>, and Bing-Joe Hwang<sup>2,3</sup>

<sup>1</sup>Department of Chemistry, Faculty of Mathematics and Natural Sciences, Institut Teknologi Sepuluh Nopember (ITS), Kampus ITS Sukolilo-Surabaya 60111, Indonesia

<sup>2</sup>Department of Chemical Engineering, National Taiwan University of Science and Technology, 43 Keelung Road, Section 4, Taipei 106, Taiwan

<sup>3</sup>National Synchrotron Radiation Research Center, Hsin-Chu 300, Taiwan

Received May 9, 2017; Accepted August 4, 2017

### ABSTRACT

The surface-modified  $\text{Na}_{2/3}\text{Co}_{2/3}\text{Mn}_{1/3}\text{O}_2$  is coated with a conductive Poly (3,4-Ethylene dioxy thiophene)-poly (styrene sulfonate) (PEDOT/PSS) polymer, and their resulting electrochemical properties were investigated as Na-ion battery cathode. The surface-modified  $\text{Na}_{2/3}\text{Co}_{2/3}\text{Mn}_{1/3}\text{O}_2$  cathode material exhibits a high discharge capacity and good rate capability due to enhanced electron transport by surface PEDOT/PSS. The presence of PEDOT/PSS surface layer suppresses the growth of a resistive layer, while the dissolution of transition metals of the active cathode materials is inhibited as well. The resulting surface-modified  $\text{Na}_{2/3}\text{Co}_{2/3}\text{Mn}_{1/3}\text{O}_2$  shows superior cycling performance, which is much stable than the pristine one as being the Na-ion battery cathode.

**Keywords:** sodium ion battery; PEDOT/PSS; cathode; surface coating

### ABSTRAK

Bahan katoda  $\text{Na}_{2/3}\text{Co}_{2/3}\text{Mn}_{1/3}\text{O}_2$  termodifikasi permukaan dilapisi dengan Polimer konduktif poly-(3,4-Ethylene dioxy tiofen)-poly (styrene sulfonate) (PEDOT/PSS), dan menghasilkan sifat elektrokimia dan digunakan sebagai katoda Na-ion baterai. Bahan katoda  $\text{Na}_{2/3}\text{Co}_{2/3}\text{Mn}_{1/3}\text{O}_2$  termodifikasi permukaan menunjukkan kapasitas discharge tinggi dan rate capability yang baik karena transpor elektron ditingkatkan oleh PEDOT/PSS permukaan. Adanya lapisan permukaan PEDOT/PSS menekan pertumbuhan lapisan resistif, sedangkan kelarutan logam transisi dari bahan katoda aktif juga dihambat.  $\text{Na}_{2/3}\text{Co}_{2/3}\text{Mn}_{1/3}\text{O}_2$  termodifikasi permukaan yang dihasilkan pada penelitian ini menunjukkan cycling performance yang tinggi, yang jauh lebih stabil daripada  $\text{Na}_{2/3}\text{Co}_{2/3}\text{Mn}_{1/3}\text{O}_2$  termodifikasi sebagai katoda baterai Na-ion.

**Kata Kunci:** baterai Na-ion; PEDOT/PSS; katoda; coating permukaan

### INTRODUCTION

The large scale applications such as electric vehicles, smart grid systems uninterruptible power supplies (UPS) for cloud computing data centers, and so on, have become a new frontier of rechargeable batteries and lead to strong demands of lithium-ion batteries, the most reliable and high energy density energy storage system to date. In such a large scale system, the cost of materials (manufacturing cost) and the cycle performance (maintenance cost) are as important as fundamental characteristics [1-3]. These demands on the lower cost electrode materials led to a rediscovery of sodium ion batteries in recent years. Na-ion technology can be a promising candidate even the associated physical and chemical properties not compatible to Li-ion one. However, it is much more

beneficial when considering the cost, the raw material abundance and the similar chemistry of Sodium and Lithium [4-5].

There are many electrode materials for sodium ion battery have been tested recently such as,  $\text{Na}_x\text{CoO}_2$  [6],  $\text{Na}_4\text{Mn}_9\text{O}_{18}$  [7],  $\text{NaFeF}_3$  [8],  $\text{NaMPO}_4$  [9],  $\text{Na}_{1.5}\text{VOPO}_4\text{F}_{0.5}$  [10],  $\text{Na}_2\text{FePO}_4\text{F}$  [11],  $\text{NaCrO}_2$  [12], carbon [13-15],  $\text{Na}_x\text{VO}_2$  [16],  $\text{Na}_2\text{Ti}_3\text{O}_7$  [17],  $\text{NaTi}_2(\text{PO}_4)_3$  [18], and  $\text{Na}_{2/3}\text{Co}_{2/3}\text{Mn}_{1/3}\text{O}_2$  [19],  $\text{Na}_3\text{V}_2(\text{PO}_4)_3$  [20] as active materials in cathodes and anodes.

Sodium lamellar oxides ( $\text{Na}_x\text{MO}_2$ ), were first studied as a positive electrode for sodium batteries in the 80's by Delmas [21-22]. The recent works of Terasaki [23] and Takada [24] put back on stage the  $\text{Na}_x\text{CoO}_2$  system due to its interesting thermoelectric properties and superconductivity of the hydrated

\* Corresponding author. Tel : +62-85732108646  
Email address : yatimnikmah@gmail.com

compound of  $\text{Na}_{0.35}\text{CoO}_2 \cdot 1.3\text{H}_2\text{O}$ . The structure of  $\text{Na}_x\text{CoO}_2$  phases can be either P2, P3,  $\text{P}\bar{3}$ , or O3. This materials become unstable because it exhibits several structure phase transition during charging/discharging. To stabilize the crystalline structure of  $\text{Na}_x\text{CoO}_2$ , Layered  $\text{Na}_{2/3}\text{Co}_{2/3}\text{Mn}_{1/3}\text{O}_2$  materials have attracted much attention as promising alternative cathode materials because it has been found that single P2-phases are formed for  $\text{Na}_{2/3}\text{Co}_{2/3}\text{Mn}_{1/3}\text{O}_2$  [19]. However, this material has poor rate capability and also cycling stability, due to decomposition of the organic electrolyte, this cathode material, test by cycling performance using 1 M  $\text{NaClO}_4$  in PC based electrolyte, and has fading until 77% for 50 cycles. To solve this problem, a number of methods have been used for enhancing the cycling stability and rate performance of ion insertion materials. Among them, carbon coating and particle size reduction are the most common strategies to enhance both the cycling stability and rate performance of cathode electrodes due to low electronic conductivity and poor ion diffusivity [11,20,56-57]. The same problem in lithium ion batteries was solved by coating the surface of cathode active materials with conductive polymers as well as inorganic materials, but in Sodium ion battery there is no report about conductive polymer coating on the electrode materials. In order to overcome this poor rate capability problem by coating the  $\text{Na}_{2/3}\text{Co}_{2/3}\text{Mn}_{1/3}\text{O}_2$  particles with various protective layers.

The surface modification of cathode materials with a conductive polymer is quite beneficial with respect to the delivery of the original capacity without a reduction of the amount of the electrochemically active element in the parent cathode materials. Among various conductive polymers, poly(3,4-ethylenedioxythiophene) (PEDOT) is one of the promising coating materials due to its high electronic conductivity and good electrochemical stability [42,44-50].

This study examines the effect on the electrochemical cycling performance of  $\text{Na}_{2/3}\text{Co}_{2/3}\text{Mn}_{1/3}\text{O}_2$  by coating its surface with the PEDOT via solution method. The treatment is expected to affect the cycle ability and also rate capability. The preparation, structure and electrochemical performance of the surface-treated  $\text{Na}_{2/3}\text{Co}_{2/3}\text{Mn}_{1/3}\text{O}_2$  cathode materials are discussed in comparison with the pristine one.

## EXPERIMENTAL SECTION

### Synthesis $\text{Na}_{2/3}\text{Co}_{2/3}\text{Mn}_{1/3}\text{O}_2$

$\text{Na}_{2/3}\text{Co}_{2/3}\text{Mn}_{1/3}\text{O}_2$  powder were prepared by a co-precipitation method using  $\text{CoSO}_4 \cdot 7\text{H}_2\text{O}$ , and  $\text{MnSO}_4 \cdot \text{H}_2\text{O}$  solution with the molar ratio of Co and Mn is 2:1, and mixed with the  $\text{Na}_2\text{CO}_3$  solution. This two solutions dropwise into batch reactor contain DI water 1

L, 60 °C, flow  $\text{CO}_2$  gas and continue stir for 12 h.  $\text{NH}_4\text{OH}$  solution was added into reactor to adjust pH = 6.7. The spherical  $\text{Co}_{2/3}\text{Mn}_{1/3}\text{CO}_3$  powders were filtered, washed with de-ionized water, and dried at 80 °C for 24 h to remove adsorbed water. A mixture of the carbonate  $\text{Co}_{2/3}\text{Mn}_{1/3}\text{CO}_3$  and  $\text{Na}_2\text{CO}_3$  with the ratio Na and precursor is 2/3:1 was mixed using 3D mixing machine. The result was preheated to 500 °C for 10 h and then heated at 950 °C for 12 h, heating rate 2 °C/min under oxygen gas flow and quench directly into room temperature [54].

### PEDOT/PSS Coated $\text{Na}_{2/3}\text{Co}_{2/3}\text{Mn}_{1/3}\text{O}_2$

PEDOT/PSS solution (Aldrich) was dispersed in N-methyl pyrrolidone (NMP) at different concentration of 3, 5, and 10 wt.%. The  $\text{Na}_{2/3}\text{Co}_{2/3}\text{Mn}_{1/3}\text{O}_2$  powders were immersed in the polymer solution, and the mixture was stirred at 60 °C for 4 h to induce surface coating of the  $\text{Na}_{2/3}\text{Co}_{2/3}\text{Mn}_{1/3}\text{O}_2$  powders. After evaporating the mixed solution and drying under vacuum at 80 °C for 24 h, the surface-modified  $\text{Na}_{2/3}\text{Co}_{2/3}\text{Mn}_{1/3}\text{O}_2$  powders were finally obtained [50].

### Electrode Preparation and Cell Assembly

The positive electrode was prepared by coating the NMP-based slurry containing surface-modified  $\text{Na}_{2/3}\text{Co}_{2/3}\text{Mn}_{1/3}\text{O}_2$  powders, poly (vinylidene fluoride) (PVdF), and super-P carbon (85:10:5 by weight) on aluminum foil. After drying under vacuum at 80 °C overnight, the electrode was punched into a disk. The geometrical area of the positive electrode was 1.54 cm<sup>2</sup>. The sodium electrode consisted of a 100 μm thick sodium foil. A CR2032-type coin cell composed of a sodium negative electrode, a glass microfiber filters separator (GF/C, Whatman), and a  $\text{Na}_{2/3}\text{Co}_{2/3}\text{Mn}_{1/3}\text{O}_2$  positive electrode was assembled with a liquid electrolyte. The liquid electrolyte used was 1 M  $\text{NaPF}_6$  in ethylene carbonate (EC)/propylene carbonate (PC) (1:1 by volume). All cells were assembled in an argon-filled dry box (Unilab, Mbruan) in which the moisture and oxygen contents were maintained less than 1 ppm [54].

### Characterization

X-ray diffraction (XRD, Bruker AXS D2, using Cu K $\alpha$  radiation) was used to identify the crystalline phase of the pristine and surface-modified  $\text{Na}_{2/3}\text{Co}_{2/3}\text{Mn}_{1/3}\text{O}_2$  powders. Fourier transform infrared (FTIR) spectra were recorded on JASCO 460 IR spectrometer using KBr pellets in the range of 400-4000 cm<sup>-1</sup>. Thermogravimetric analysis (TGA) was conducted on simultaneous TGA/DSC analyzer (SDT Q500, TA

Instrument) at a heating rate of 5 °C/min under N<sub>2</sub> and O<sub>2</sub> flow. AC impedance measurement was then performed to measure ionic conductivity using an impedance analyzer over the frequency range of 100 mHz to 1 MHz with an amplitude of 10 mV. Charge and discharge cycling tests of the Na/Na<sub>2/3</sub>Co<sub>2/3</sub>Mn<sub>1/3</sub>O<sub>2</sub> cells were conducted at different current densities over the voltage range of 1.25–4.3 V using battery testing equipment (Arbin machine).

## RESULT AND DISCUSSION

To determine if any unexpected effect of PEDOT coating on the crystalline structure of Na<sub>2/3</sub>Co<sub>2/3</sub>Mn<sub>1/3</sub>O<sub>2</sub>, the X-ray powder diffraction was carried out for uncoated and coated Na<sub>2/3</sub>Co<sub>2/3</sub>Mn<sub>1/3</sub>O<sub>2</sub> materials. The XRD patterns of the bare and PEDOT coated Na<sub>2/3</sub>Co<sub>2/3</sub>Mn<sub>1/3</sub>O<sub>2</sub> in different concentration are presented in Fig. 1.

The XRD patterns of the bare Na<sub>2/3</sub>Co<sub>2/3</sub>Mn<sub>1/3</sub>O<sub>2</sub> and PEDOT-coated Na<sub>2/3</sub>Co<sub>2/3</sub>Mn<sub>1/3</sub>O<sub>2</sub> are shown in Fig. 1. All the diffractions were indexed to hexagonal structure, pure P2 phase with space group of P6<sub>3</sub>/mmc [19]. There is no significant change in the XRD patterns for the Na<sub>2/3</sub>Co<sub>2/3</sub>Mn<sub>1/3</sub>O<sub>2</sub> materials after PEDOT/PSS coating, indicating no side reaction between the polymeric coating and Na<sub>2/3</sub>Co<sub>2/3</sub>Mn<sub>1/3</sub>O<sub>2</sub>.

To understand the weight percentage of PEDOT/PSS in the coated Na<sub>2/3</sub>Co<sub>2/3</sub>Mn<sub>1/3</sub>O<sub>2</sub>, the associated TGA data of the bare Na<sub>2/3</sub>Co<sub>2/3</sub>Mn<sub>1/3</sub>O<sub>2</sub> powder and the coated Na<sub>2/3</sub>Co<sub>2/3</sub>Mn<sub>1/3</sub>O<sub>2</sub> with various PEDOT weight percentages are shown in Fig. 2. The PEDOT composition are comparatively, more the product is rich in polymer more it is degraded easily. Higher percentage of PEDOT, give higher weight losses.

As shown in Fig. 2, it can be clearly observed that there were three-step weight losses for all three different PEDOT/PSS content. The polymers initially underwent a small weight decrease at relatively low temperature around 120 °C, which may be attributed to moisture evaporation. With the gradual increasing of the temperature, another weight loss was found at 300 °C, which were essentially due to the oxidizing decomposition of the skeletal PEDOT backbone chain structures. The last step weight loss at temperatures 500 °C should be attributed to the thermal decomposition of NaClO<sub>4</sub>.

The existence of PEDOT on the Na<sub>2/3</sub>Co<sub>2/3</sub>Mn<sub>1/3</sub>O<sub>2</sub> particle was further confirmed by comparison of the FTIR spectra of pristine and surface-modified Na<sub>2/3</sub>Co<sub>2/3</sub>Mn<sub>1/3</sub>O<sub>2</sub> particles. As shown in Fig. 3, the pristine Na<sub>2/3</sub>Co<sub>2/3</sub>Mn<sub>1/3</sub>O<sub>2</sub> particle exhibits a broad band around 540 cm<sup>-1</sup> [50], which comes from the M–O vibration [51-52]. No significant shift could be observed after polymer coating in this region, indicating no strong

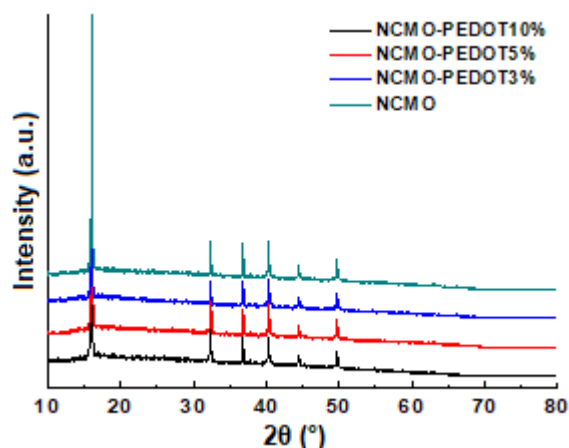


**Fig 1.** X-ray diffraction patterns of Na<sub>2/3</sub>Co<sub>2/3</sub>Mn<sub>1/3</sub>O<sub>2</sub> and the PEDOT-coated Na<sub>2/3</sub>Co<sub>2/3</sub>Mn<sub>1/3</sub>O<sub>2</sub> in different concentration

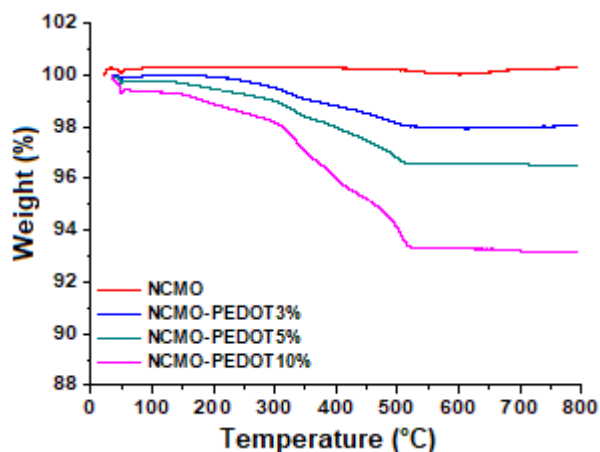


**Fig 2.** TGA curve of Na<sub>2/3</sub>Co<sub>2/3</sub>Mn<sub>1/3</sub>O<sub>2</sub> and the PEDOT-coated Na<sub>2/3</sub>Co<sub>2/3</sub>Mn<sub>1/3</sub>O<sub>2</sub> in different concentration

interactions between PEDOT and Na<sub>2/3</sub>Co<sub>2/3</sub>Mn<sub>1/3</sub>O<sub>2</sub>. The presence of PEDOT could be confirmed by the C=C ring and C–O–R vibration in PEDOT at about 1120 cm<sup>-1</sup> [42,53].

The CV (cyclic voltammetry) was conducted for the pristine Na<sub>2/3</sub>Co<sub>2/3</sub>Mn<sub>1/3</sub>O<sub>2</sub> and PEDOT-coated Na<sub>2/3</sub>Co<sub>2/3</sub>Mn<sub>1/3</sub>O<sub>2</sub> with different PEDOT content. From the CV curve (Fig. 4) with different concentration of PEDOT, it is seen all the PEDOT content exhibit four couple of peak in the anodic and cathodic sweeps. This suggests that the intercalation and deintercalation of sodium ions were carried out in four steps. The cathodic and anodic peaks show different phase formation of Na<sub>2/3</sub>Co<sub>2/3</sub>Mn<sub>1/3</sub>O<sub>2</sub>. The first peak in 4 V is the formation of Na<sub>x</sub>Co<sub>2/3</sub>Mn<sub>1/3</sub>O<sub>2</sub>, for x = 0.3439. The second redox peak couple in 3.55 V is another phase change, x = 0.5. The other redox peaks couple in 3.4 V, 2.5 V and 1.5 V are the phase change for x = 0.52, 0.67 and 0.87, respectively. This behavior was

observed with the previous work [19]. The redox pairs of Co and Mn also contribute in the cathode materials. Its agree with our previous research [54] that the discharging process for both the Co and the Mn, suggesting that the redox pairs, that is,  $\text{Co}^{3+}/\text{Co}^{2+}$  and  $\text{Mn}^{4+}/\text{Mn}^{3+}$ , are both involved in the reaction.

The cathodic and anodic peaks in the PEDOT/PSS 3% shows the irreversible shift (Fig. 4) from 4.17 V to 3.85 and other anodic and cathodic peak in 3.8 V to 3.5 V suggests that the structural change happen. In contrast, for the Pristine and other PEDOT/PSS content 5% and 10%, there is no sign of any irreversible structural change.

These CV data are in good agreement with the discharge/charge curves in Fig. 5. In the cycling profile, the significant peaks that can be seen in the CV can be observed as well. The dominating feature is the plateau around 4 V, 3.5 V, 2.5 V and 1.5 V.

In order to evaluate the influence of PEDOT/PSS content on the electrochemical performance of the pristine and PEDOT-coated  $\text{Na}_{2/3}\text{Co}_{2/3}\text{Mn}_{1/3}\text{O}_2$ , CR2032 coin-type cells were fabricated using Na foil as the counter electrode and 1 M  $\text{NaPF}_6$  in EC/PC (1:1 by volume) as the electrolyte. Fig. 5 presents the cell voltage versus specific capacity curves for the 1<sup>st</sup> to 5<sup>th</sup> cycles of  $\text{Na}_{2/3}\text{Co}_{2/3}\text{Mn}_{1/3}\text{O}_2$  and PEDOT-coated  $\text{Na}_{2/3}\text{Co}_{2/3}\text{Mn}_{1/3}\text{O}_2$  with different PEDOT contents in the voltage range of 1.25 to 4.3 V at a constant current rate

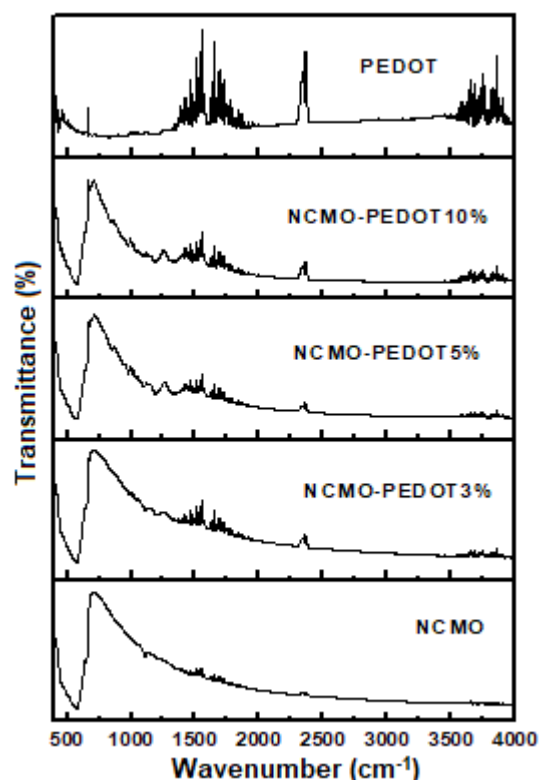


**Fig 3.** FTIR spectra of  $\text{Na}_{2/3}\text{Co}_{2/3}\text{Mn}_{1/3}\text{O}_2$  and the PEDOT-coated  $\text{Na}_{2/3}\text{Co}_{2/3}\text{Mn}_{1/3}\text{O}_2$  in different concentration

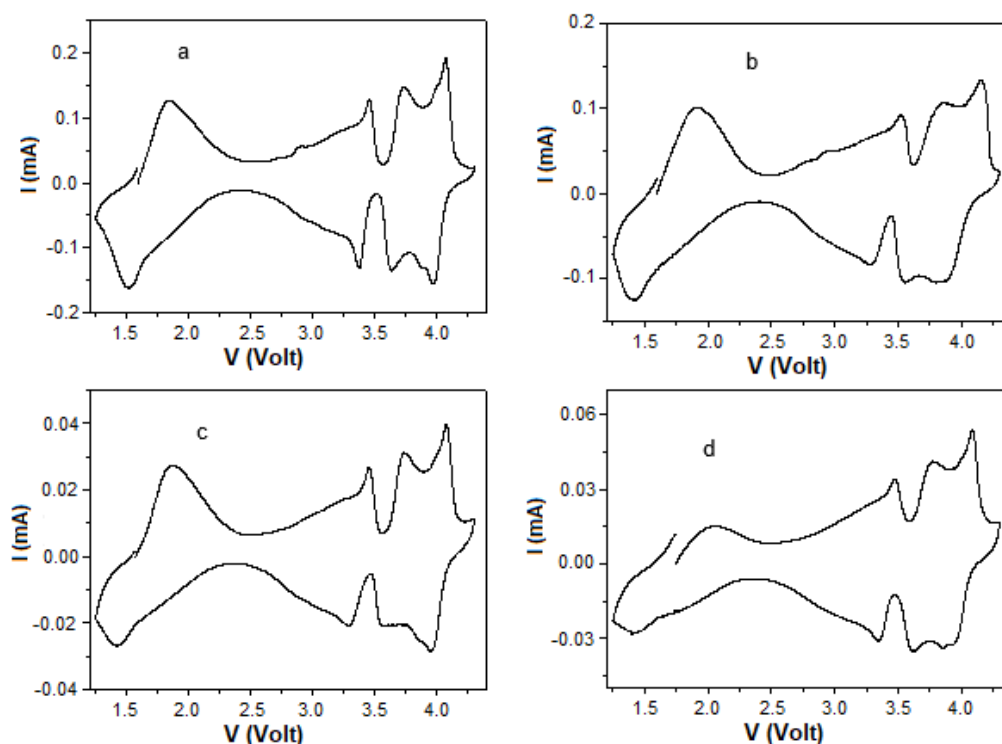


**Fig 4.** Cyclic Voltammetry curve of  $\text{Na}_{2/3}\text{Co}_{2/3}\text{Mn}_{1/3}\text{O}_2$  and the PEDOT-coated  $\text{Na}_{2/3}\text{Co}_{2/3}\text{Mn}_{1/3}\text{O}_2$  in different PEDOT/PSS content: a) 0 wt.%, b) 3 wt.%, c) 5 wt.%, and d) 10 wt.%

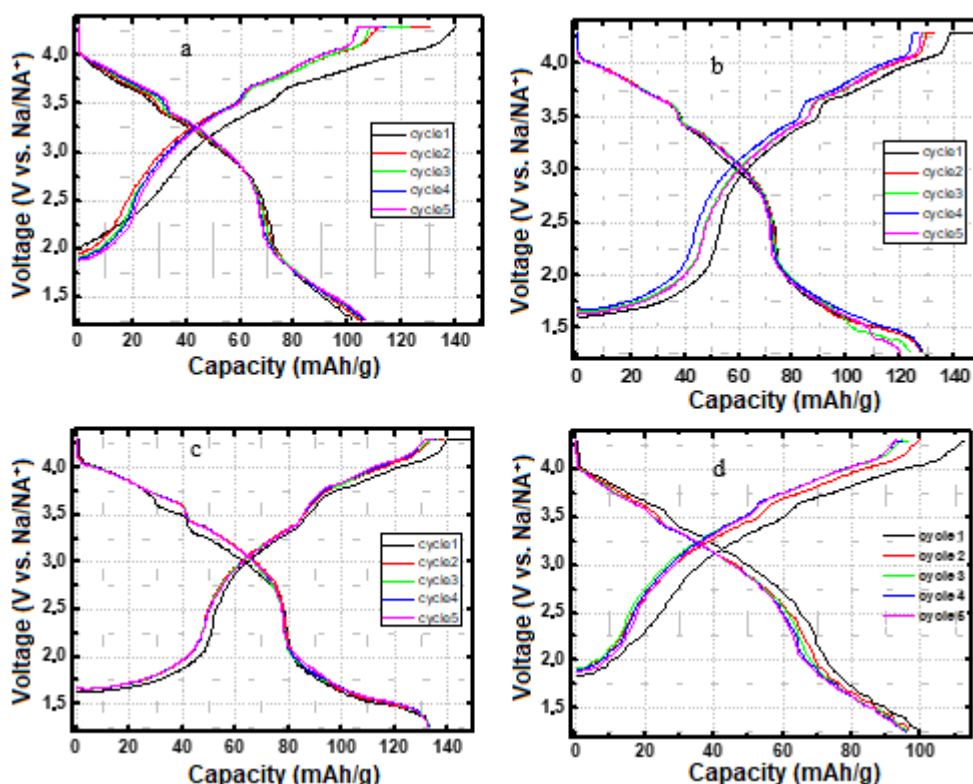


**Fig 5.** Charge – discharge curve of  $\text{Na}_{2/3}\text{Co}_{2/3}\text{Mn}_{1/3}\text{O}_2$  and the PEDOT-coated  $\text{Na}_{2/3}\text{Co}_{2/3}\text{Mn}_{1/3}\text{O}_2$  in different PEDOT/PSS content : a) 0 wt.%, b) 3 wt.%, c) 5wt.%, and d) 10 wt.%

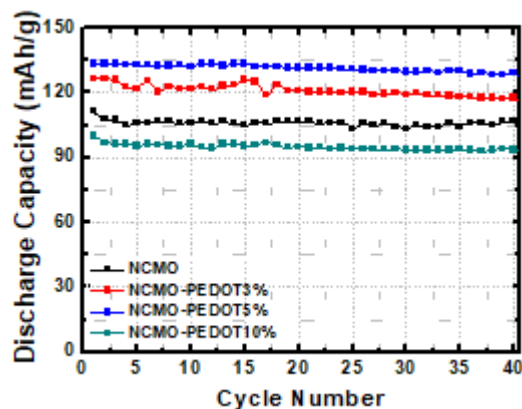


**Fig 6.** Cycling performance of  $\text{Na}_{2/3}\text{Co}_{2/3}\text{Mn}_{1/3}\text{O}_2$  and the PEDOT-coated  $\text{Na}_{2/3}\text{Co}_{2/3}\text{Mn}_{1/3}\text{O}_2$  with different PEDOT/PSS content at the rate 0.1C and scan range 1.25 – 4.3 V

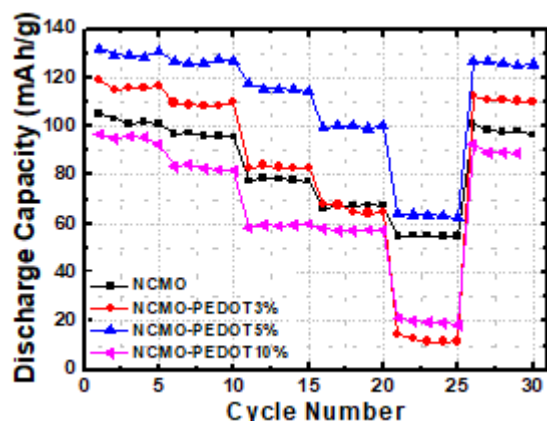
of 0.1 C. The cells were galvanostatically charged and discharged repeatedly at the rate 0.1 C between 1.25 V and 4.3 V at room temperature. From Fig. 5, it is seen that for the  $\text{Na}_{2/3}\text{Co}_{2/3}\text{Mn}_{1/3}\text{O}_2$  and PEDOT-coated  $\text{Na}_{2/3}\text{Co}_{2/3}\text{Mn}_{1/3}\text{O}_2$  with different PEDOT content, there are four charge plateaus at 4; 3.55; 2.67 and 1.45 V as well as four discharge plateaus at 4.1; 3.7; 2.7; and 1.75 V, which agrees with the CV results (Fig. 4). It also the same result with the previous work [54].

The PEDOT coated  $\text{Na}_{2/3}\text{Co}_{2/3}\text{Mn}_{1/3}\text{O}_2$  with PEDOT content 10% exhibits the lowest initial discharge capacity of 100.06 mAh/g, compare with  $\text{Na}_{2/3}\text{Co}_{2/3}\text{Mn}_{1/3}\text{O}_2$  and other PEDOT-coated  $\text{Na}_{2/3}\text{Co}_{2/3}\text{Mn}_{1/3}\text{O}_2$  sample. The PEDOT-coated  $\text{Na}_{2/3}\text{Co}_{2/3}\text{Mn}_{1/3}\text{O}_2$  with the PEDOT content 10% shows the worse discharge capacity due to the PEDOT on the surface to much, so the sodium intercalation from active material was inhibit by PEDOT (the coating to thick). In contrast, the PEDOT-coated  $\text{Na}_{2/3}\text{Co}_{2/3}\text{Mn}_{1/3}\text{O}_2$  with 5 wt.% PEDOT exhibits the highest initial discharge capacity of 133.55 mAh/g. The conductive polymer coating is expected to reduce the contact resistance between the active cathode particles and facilitate electron transport in the positive electrode. It is also plausible that the PEDOT layer can provide reversible capacity as a cathode active material. As a result, the  $\text{Na}_{2/3}\text{Co}_{2/3}\text{Mn}_{1/3}\text{O}_2$  cathode material coated by the PEDOT exhibited a higher discharge capacity.

The capacity retention was also improved when using the PEDOT-coated  $\text{Na}_{2/3}\text{Co}_{2/3}\text{Mn}_{1/3}\text{O}_2$  electrode. The capacity loss of the surface-modified  $\text{Na}_{2/3}\text{Co}_{2/3}\text{Mn}_{1/3}\text{O}_2$  electrode by PEDOT was only 2.8% after 40 cycles, while the pristine electrode suffered a 6% capacity loss (Fig. 6). The good capacity retention in the cell with the surface-modified  $\text{Na}_{2/3}\text{Co}_{2/3}\text{Mn}_{1/3}\text{O}_2$

**Table 1.** Efficiency and capacity retention of  $\text{Na}_{2/3}\text{Co}_{2/3}\text{Mn}_{1/3}\text{O}_2$  and PEDOT-coated  $\text{Na}_{2/3}\text{Co}_{2/3}\text{Mn}_{1/3}\text{O}_2$  with different PEDOT content at the rate 0.5C and scan range 1.25–4.3 V

Sample name	1 <sup>st</sup> charge capacity (mAh/g)	1 <sup>st</sup> discharge capacity (mAh/g)	Efficiency 1 <sup>st</sup> cycle (%)	100 <sup>th</sup> discharge capacity (mAh/g)	Capacity retention (%)
Pristine	84.29366	79.35233	94	56.69337	70
PEDOT/PSS 3%	91.74377	87.55316	95	61.29334	71
PEDOT/PSS 5%	127.58791	123.82171	97	103.98194	84
PEDOT/PSS 10%	74.31743	67.65846	91	53.41046	79

**Fig 7.** Rate capability of  $\text{Na}_{2/3}\text{Co}_{2/3}\text{Mn}_{1/3}\text{O}_2$  and the PEDOT-coated  $\text{Na}_{2/3}\text{Co}_{2/3}\text{Mn}_{1/3}\text{O}_2$  with different PEDOT/PSS content at the rate 0.1C and scan range 1.25–4.3 V

particles can be ascribed to the presence of a conductive polymer film on the active sites of the cathode.

This conductive polymer film functions as a protective layer to cover the active cathode sites and reduce the oxidative decomposition of the electrolyte, such that the structural stability of cathode material can be enhanced. This result suggests that the surface coating conductive polymer is more effective for high discharge capacity and good capacity retention.

Fig. 7 shows the Rate capability of  $\text{Na}_{2/3}\text{Co}_{2/3}\text{Mn}_{1/3}\text{O}_2$  and the PEDOT-coated  $\text{Na}_{2/3}\text{Co}_{2/3}\text{Mn}_{1/3}\text{O}_2$  with different PEDOT/PSS content. The PEDOT-coated  $\text{Na}_{2/3}\text{Co}_{2/3}\text{Mn}_{1/3}\text{O}_2$  delivered higher discharge capacities at high C rates, and 5% PEDOT-coated  $\text{Na}_{2/3}\text{Co}_{2/3}\text{Mn}_{1/3}\text{O}_2$  delivered the highest discharge capacity in the same rate. For example, the PEDOT-coated  $\text{Na}_{2/3}\text{Co}_{2/3}\text{Mn}_{1/3}\text{O}_2$  with the PEDOT content 0%, 3%, 5% and 10% delivered a discharge capacity of 66.58, 67.85, 100.27, and 58.01 mAh/g at 1 C rate, respectively. By coating a conductive polymer on the surface of the cathode material, the electronic conductivity was improved, which facilitates the charge transfer reaction. In this way, the PEDOT acts as a conducting network that increases the rate of electron in the depth of the electrode.

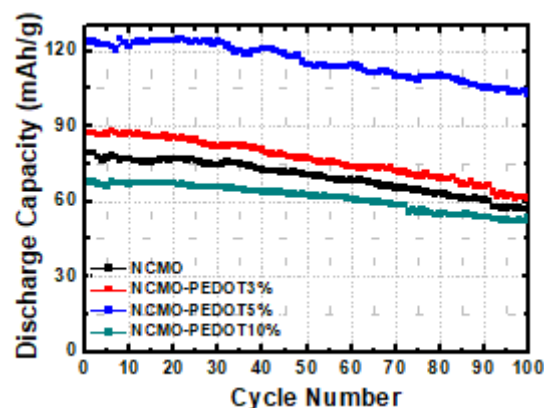
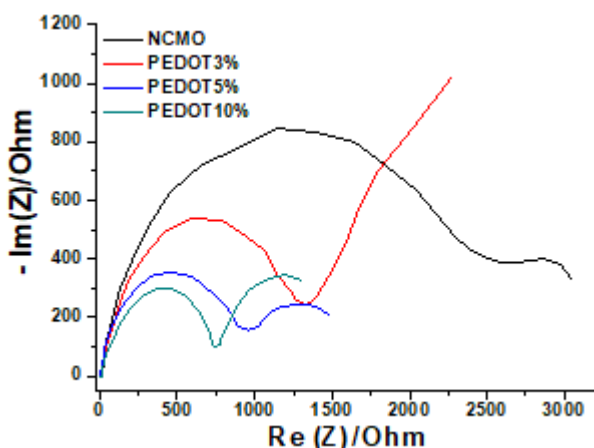
**Fig 8.** Cycling performance of  $\text{Na}_{2/3}\text{Co}_{2/3}\text{Mn}_{1/3}\text{O}_2$  and the PEDOT-coated  $\text{Na}_{2/3}\text{Co}_{2/3}\text{Mn}_{1/3}\text{O}_2$  with different PEDOT/PSS content at the rate 0.5C and scan range 1.25–4.3 V

Fig. 8 shows the cycling performance of  $\text{Na}_{2/3}\text{Co}_{2/3}\text{Mn}_{1/3}\text{O}_2$  and the PEDOT-coated  $\text{Na}_{2/3}\text{Co}_{2/3}\text{Mn}_{1/3}\text{O}_2$  with different PEDOT/PSS content in the high C rate, 0.5 C. The same behavior was observed with the smaller C rate, 0.1 C. The comparison of the result can be seen in Table 1. From Table 1, it showed the comparison about the efficiency in first cycle and capacity retention after 100 cycles for all sample. The PEDOT-coated  $\text{Na}_{2/3}\text{Co}_{2/3}\text{Mn}_{1/3}\text{O}_2$  with 5 wt.% PEDOT exhibits the highest efficiency and also capacity retention after 100 cycles in the high C rate, 0.5 C.

In order to understand the effect of the PEDOT on the ac impedance behavior of the  $\text{Na}/\text{Na}_{2/3}\text{Co}_{2/3}\text{Mn}_{1/3}\text{O}_2$  cells, ac impedance measurements were performed after cycling at room temperature. The ac impedances of the cells were measured after 5 cycles, and the resultant ac impedance spectra are shown in Fig. 9. In all the cells, it observed the semicircle in the high frequency range that can be attributed to the resistance due to  $\text{Na}^+$  ion migration through the surface film on the electrode ( $R_f$ ), while the semicircle observed in the medium-to-low frequency range is due to the charge transfer resistance between the electrode and electrolyte ( $R_{ct}$ ) [55-56]. Both surface film resistance and charge transfer resistance in the cell with the



**Fig 9.** Nyquist plots of  $\text{Na}_{2/3}\text{Co}_{2/3}\text{Mn}_{1/3}\text{O}_2$  and the PEDOT-coated  $\text{Na}_{2/3}\text{Co}_{2/3}\text{Mn}_{1/3}\text{O}_2$  in different PEDOT/PSS content

PEDOT coated  $\text{Na}_{2/3}\text{Co}_{2/3}\text{Mn}_{1/3}\text{O}_2$  material are lower than those of the cells containing pristine  $\text{Na}_{2/3}\text{Co}_{2/3}\text{Mn}_{1/3}\text{O}_2$ . By increasing the PEDOT content, the  $R_f$  and  $R_{ct}$  also decrease. This supports the notion that a protective conductive polymer layer on the cathode limits the growth of a resistive layer due to the oxidative decomposition of electrolyte. A conductive polymer layer on the surface of the active material would also produce good electrical contact between the less conductive  $\text{Na}_{2/3}\text{Co}_{2/3}\text{Mn}_{1/3}\text{O}_2$  particles as well as give rise to protection of the cathode particle from HF attack, which facilitates electron transfer. These results indicate that the surface modification of the  $\text{Na}_{2/3}\text{Co}_{2/3}\text{Mn}_{1/3}\text{O}_2$  active materials by the conductive PEDOT layer is very effective for reducing interfacial resistances during cycling.

## CONCLUSION

The  $\text{Na}_{2/3}\text{Co}_{2/3}\text{Mn}_{1/3}\text{O}_2$  cathode materials were synthesized and surface-modified by coating with a conductive PEDOT copolymer. The surface modified  $\text{Na}_{2/3}\text{Co}_{2/3}\text{Mn}_{1/3}\text{O}_2$  cathode material delivered a higher initial discharge capacity and exhibited more stable cycling characteristics than the pristine  $\text{Na}_{2/3}\text{Co}_{2/3}\text{Mn}_{1/3}\text{O}_2$  materials. The presence of the conductive polymer layer formed on the cathode enhanced the high rate performance due to enhanced transport of electrons as well as good electrical contact between the  $\text{Na}_{2/3}\text{Co}_{2/3}\text{Mn}_{1/3}\text{O}_2$  particles. It can be concluded that the surface modification of the  $\text{Na}_{2/3}\text{Co}_{2/3}\text{Mn}_{1/3}\text{O}_2$  cathode materials with the PEDOT/PSS polymer provides a high reversible capacity, stable cycling characteristics, and good rate capability.

## ACKNOWLEDGEMENT

The financial supports from the Ministry of Science and Technology (MOST) (103-3113-E-011-001, 101-3113-E-011-002, 101-2923-E-011-001-MY3, 100-2221-E-011-105-MY3), the Ministry of Economic Affairs (MOEA) (101-EC-17-A-08-S1-183), and the Top University Projects of Ministry of Education (MOE) (100H451401), as well as the facilities supports from the National Taiwan University of Science and Technology (NTUST) are acknowledged.

## REFERENCES

- [1] Armand, M., and Tarascon, J.M., 2008, Building better batteries, *Nature*, 451 (7179), 652–657.
- [2] Zu, C.X., and Li, H., 2011, Thermodynamic analysis on energy densities of batteries, *Energy Environ. Sci.*, 4 (8), 2614–2624.
- [3] Yang, Z., Zhang, J., Kintner-Meyer, M.C.W., Lu, X., Choi, D., Lemmon, J.P., and Liu, J., 2011, Electrochemical energy storage for green grid, *Chem. Rev.*, 111 (5), 3577–3613.
- [4] Palomares, V., Serras, P., Villaluenga, I., Hueso, K.B., Carretero-González, J., and Rojo, T., 2012, Na-ion batteries, recent advances and present challenges to become low cost energy storage systems, *Energy Environ. Sci.*, 5, 5884–5901.
- [5] Wang, L., Lu, Y., Liu, J., Xu, M., Cheng, J., Zhang, D., and Goodenough, J.B., 2013, A superior low-cost cathode for a Na-ion battery, *Angew. Chem. Int. Ed.*, 52, 1964–1967.
- [6] Berthelot, R., Carlier, D., and Delmas, C., 2011, Electrochemical investigation of  $\text{P2-Na}_x\text{CoO}_2$  phase diagram, *Nat. Mater.*, 10 (1), 74–80.
- [7] Cao, Y., Xiao, L., Wang, W., Choi, D., Nie, Z., Yu, J., Saraf, L.V., Yang, Z., and Liu, J., 2011, Reversible sodium ion insertion in single crystalline manganese oxide nanowires with long cycle life, *Adv. Mater.*, 23 (28), 3155–3160.
- [8] Yamada, Y., Doi, T., Tanaka, I., Okada, S., and Yamaki, J., 2011, Liquid-phase synthesis of highly dispersed  $\text{NaFeF}_3$  particles and their electrochemical properties for sodium-ion batteries, *J. Power Sources*, 196 (10), 4837–4841.
- [9] Lee, K.T., Ramesh, T.N., Nan, F., Botton, G., and Nazar, L.F., 2011, Topochemical synthesis of sodium metal phosphate olivines for sodium-ion batteries, *Chem. Mater.*, 23 (16), 3593–3600.
- [10] Sauvage, F., Quarez, E., Tarascon, J.M., and Baudrin, E., 2006, Crystal structure and electrochemical properties vs.  $\text{Na}^+$  of the sodium fluorophosphate  $\text{Na}_{1.5}\text{VOPO}_4\text{F}_{0.5}$ , *Solid State Sci.*, 8 (10), 1215–1221.

- [11] Kawabe, Y., Yabuuchi, N., Kajiyama, M., Fukuhara, N., Inamasu, T., Okuyama, R., Nakai, I., and Komaba, S., 2011, Synthesis and electrode performance of carbon coated  $\text{Na}_2\text{FePO}_4\text{F}$  for rechargeable Na batteries, *Electrochem. Commun.*, 13 (11), 1225–1228.
- [12] Komaba, S., Nakayama, T., Ogata, A., Shimizu, T., Takei, C., Takada, S., Hokura, A., and Nakai, I., 2009, Electrochemically reversible sodium intercalation of layered  $\text{NaNi}_{0.5}\text{Mn}_{0.5}\text{O}_2$  and  $\text{NaCrO}_2$ , *ECS Trans.*, 16 (42), 43–55.
- [13] Komaba, S., Murata, W., Ishikawa, T., Yabuuchi, N., Ozeki, T., Nakayama, T., Ogata, A., Gotoh, K., and Fujiwara, K., 2011, Electrochemical Na insertion and solid electrolyte interphase for hard-carbon electrodes and application to Na-ion batteries, *Adv. Funct. Mater.*, 21 (20), 3859–3867.
- [14] Wenzel, S., Hara, T., Janek, J., and Adelhelm, P., 2011, Room-temperature sodium-ion batteries: Improving the rate capability of carbon anode materials by templating strategies, *Energy Environ. Sci.*, 4, 3342–3345.
- [15] Stevens, D.A., and Dahn, J.R., 2000, High capacity anode materials for rechargeable sodium-ion batteries, *J. Electrochem. Soc.*, 147 (4), 1271–1273.
- [16] Hamani, D., Ati, M., Tarascon, J.M., and Rozier, P., 2011,  $\text{Na}_x\text{VO}_2$  as possible electrode for Na-ion batteries, *Electrochem. Commun.*, 13 (9), 938–941.
- [17] Senguttuvan, P., Rousse, G., Seznec, V., Tarascon, J.M., and Palacin, M.R., 2011,  $\text{Na}_2\text{Ti}_3\text{O}_7$ : Lowest voltage ever reported oxide insertion electrode for sodium ion batteries, *Chem. Mater.*, 23 (18), 4109–4111.
- [18] Park, S.I. Gocheva, I., Okada, S., and Yamaki, J., 2011, Electrochemical properties of  $\text{NaTi}_2(\text{PO}_4)_3$  anode for rechargeable aqueous sodium-ion batteries, *J. Electrochem. Soc.*, 158 (10), A1067–A1070.
- [19] Carlier, D., Cheng, J.H., Berthelot, R., Guignard, M., Yoncheva, M., Stoyanova, R., Hwang, B.J., and Delmas, C., 2011, The  $\text{P2-Na}_{2/3}\text{Co}_{2/3}\text{Mn}_{1/3}\text{O}_2$  phase: Structure, physical properties and electrochemical behavior as positive electrode in sodium battery, *Dalton Trans.*, 40 (36), 9306–9312.
- [20] Jian, Z., Zhao, L., Pan, H., Hu, Y.S., Li, H., Chen, W., and Chen, L., 2012, Carbon coated  $\text{Na}_3\text{V}_2(\text{PO}_4)_3$  as novel electrode material for sodium ion batteries, *Electrochem. Commun.*, 14 (1), 86–89.
- [21] Braconnier, J.J., Delmas, C., Fouassier, C., and Hagenmuller, P., 1980, Comportement electrochimique des phases  $\text{Na}_x\text{CoO}_2$ , *Mater. Res. Bull.*, 15 (12), 1797–1804.
- [22] Delmas, C., Braconnier, J.J., Fouassier, C., and Hagenmuller, P., 1981, Electrochemical intercalation of sodium in  $\text{Na}_x\text{CoO}_2$  bronzes, *Solid State Ionics*, 3-4, 165–169.
- [23] Terasaki, I., Sasago, Y., and Uchinokura, K., 1997, Large thermoelectric power in  $\text{NaCo}_2\text{O}_4$  single crystals, *Phys. Rev. B*, 56 (20), R12685–R12687.
- [24] Takada, K., Sakurai, H., Takayama-Muromachi, E., Izumi, F., Dilanian, R.A., and Sasaki, T., 2003, Superconductivity in two-dimensional  $\text{CoO}_2$  layers, *Nature*, 422 (6927), 53–55.
- [25] Cho, J., Kim, Y.J., Kim, T.J., and Park, B., 2001, Zero-strain intercalation cathode for rechargeable Li-ion cell, *Angew. Chem. Int. Ed.*, 40 (18), 3367–3369.
- [26] Gnanaraj, J.S., Pol, V.G., Gedanken, A., and Aurbach, D., 2003, Improving the high-temperature performance of  $\text{LiMn}_2\text{O}_4$  spinel electrodes by coating the active mass with MgO via a sonochemical method, *Electrochem. Commun.*, 5 (11), 940–945.
- [27] Chen, Z., Qin, Y., Amine, K., and Sun, Y.K., 2010, Role of surface coating on cathode materials for lithium-ion batteries, *J. Mater. Chem.*, 20, 7606–7612.
- [28] Fan, Y., Wang, J., Tang, Z., He, W., and Zhang, J., 2007, Effects of the nanostructured  $\text{SiO}_2$  coating on the performance of  $\text{LiNi}_{0.5}\text{Mn}_{1.5}\text{O}_4$  cathode materials for high-voltage Li-ion batteries, *Electrochim. Acta*, 52 (11), 3870–3875.
- [29] Woo, S.U., Yoon, C.S., Amine, K., Belharouak, I., and Sun, Y.K., 2007, Significant improvement of electrochemical performance of  $\text{AlF}_3$ -coated  $\text{Li}[\text{Ni}_{0.8}\text{Co}_{0.1}\text{Mn}_{0.1}]\text{O}_2$  cathode materials, *J. Electrochem. Soc.*, 154 (11), A1005–A1009.
- [30] Myung, S.T., Amine, K., and Sun, Y.K., 2010, Surface modification of cathode materials from nano- to microscale for rechargeable lithium-ion batteries, *J. Mater. Chem.*, 20, 7074–7095.
- [31] Sclar, H., Haik, O., Menachem, T., Grinblat, J., Leifer, N., Meitav, A., Luski, S., and Aurbach, D., 2012, The effect of ZnO and MgO coatings by a sono-chemical method, on the stability of  $\text{LiMn}_{1.5}\text{Ni}_{0.5}\text{O}_4$  as a cathode material for 5 V Li-ion batteries, *J. Electrochem. Soc.*, 159 (3), A228–A237.
- [32] Arbizzani, C., Mastragostino, M., and Rossi, M., 2002, Preparation and electrochemical characterization of a polymer  $\text{Li}_{1.03}\text{Mn}_{1.97}\text{O}_4/\text{pEDOT}$  composite electrode, *Electrochem. Commun.*, 4 (7), 545–549.
- [33] Arbizzani, C., Balducci, A., Mastragostino, M., Rossi, M., and Soavi, F., 2003,  $\text{Li}_{1.01}\text{Mn}_{1.97}\text{O}_4$  surface modification by poly(3,4-

- ethylenedioxythiophene), *J. Power Sources*, 119-121, 695–700.
- [34] Wang, G.X., Yang, L., Chen, Y., Wang, J.Z., Bewlay, S., and Liu, H.K., 2005, An investigation of polypyrrole-LiFePO<sub>4</sub> composite cathode materials for lithium-ion batteries, *Electrochim. Acta*, 50 (24), 4649–4654.
- [35] Huang, Y.H., Park, K.S., and Goodenough, J.B., 2006, Improving lithium batteries by tethering carbon-coated LiFePO<sub>4</sub> to polypyrrole, *J. Electrochem. Soc.*, 153 (12), A2282–A2286.
- [36] Her, L.J., Hong, J.L., and Chang, C.C., 2006, Preparation and electrochemical characterizations of poly(3,4-dioxyethylenethiophene)/LiCoO<sub>2</sub> composite cathode in lithium-ion battery, *J. Power Sources*, 157 (1), 457–463.
- [37] Park, K.S., Schougaard, S.B., and Goodenough, J.B., 2007, Conducting-polymer/iron-redox-couple composite cathodes for lithium secondary batteries, *Adv. Mater.*, 19 (6), 848–851.
- [38] Lee, K.S., Sun, Y.K., Noh, J., Song, K.S., and Kim, D.W., 2009, Improvement of high voltage cycling performance and thermal stability of lithium-ion cells by use of a thiophene additive, *Electrochem. Commun.*, 11 (10), 1900–1903.
- [39] Fedorková, A., Oriňáková, R., Orinák, A., Talian, I., Heile, A., Wiemhöfer, H.D., Kaniánsky, D., and Arlinghaus, H.F., 2010, PPy doped PEG conducting polymer films synthesized on LiFePO<sub>4</sub> particles, *J. Power Sources*, 195, 3907–3912.
- [40] Fedorková, A., Oriňáková, R., Orinák, A., Wiemhöfer, H.D., Kaniánsky, D., and Winter, M., 2010, Surface treatment of LiFePO<sub>4</sub> cathode material with PPy/PEG conductive layer, *J. Solid State Electrochem.*, 14 (12), 2173–2178.
- [41] Sinha, N.N., and Munichandraiah, N., 2009, Synthesis and characterization of carbon-coated LiNi<sub>1/3</sub>Co<sub>1/3</sub>Mn<sub>1/3</sub>O<sub>2</sub> in a single step by an inverse microemulsion route, *ACS Appl. Mater. Interfaces*, 1 (6), 1241–1249.
- [42] Lepage, D., Michot, C., Liang, G., Gauthier, M., and Schougaard, S.B., 2011, A soft chemistry approach to coating of LiFePO<sub>4</sub> with a conducting polymer, *Angew. Chem. Int. Ed.*, 50 (30), 6884–6887.
- [43] Zhan, L., Song, Z., Zhang, J., Tang, J., Zhan, H., Zhou, Y., and Zhan, C., 2008, PEDOT: Cathode active material with high specific capacity in novel electrolyte system, *Electrochim. Acta*, 53 (28), 8319–8323.
- [44] Lee, Y.S., Lee, K.S., Sun, Y.K., Lee, Y.M., and Kim, D.W., 2011, Effect of an organic additive on the cycling performance and thermal stability of lithium-ion cells assembled with carbon anode and LiNi<sub>1/3</sub>Co<sub>1/3</sub>Mn<sub>1/3</sub>O<sub>2</sub> cathode, *J. Power Sources*, 196 (16), 6997–7001.
- [45] Yao, Y., Liu, N., McDowell, M.T., Pasta, M., and Cui, Y., 2012, Improving the cycling stability of silicon nanowire anodes with conducting polymer coatings, *Energy Environ. Sci.*, 5, 7927–7930.
- [46] Zhou, J., and Lubineau, G., 2013, Improving Electrical Conductivity in Polycarbonate Nanocomposites Using Highly Conductive PEDOT/PSS Coated MWCNTs, *ACS Appl. Mater. Interfaces*, 5 (13), 6189–6200.
- [47] Dziewoński, P.M., and Grzeszczuk, M., 2010, Towards TiO<sub>2</sub>-conducting polymer hybrid materials for lithium ion batteries, *Electrochim. Acta*, 55 (9), 3336–3347.
- [48] Yang, Y., Yu, G., Cha, J.J., Wu, H., Vosgueritchian, M., Yao, Y., Bao, Z., and Cui, Y., 2011, Improving the performance of lithium–sulfur batteries by conductive polymer coating, *ACS Nano*, 5 (11), 9187–9193.
- [49] Ju, S.H., Kang, I.S., Lee, Y.S., Shin, W.K., Kim, S., Shin, K., and Kim, D.W., 2014, Improvement of the cycling performance of LiNi<sub>0.6</sub>Co<sub>0.2</sub>Mn<sub>0.2</sub>O<sub>2</sub> cathode active materials by a dual-conductive polymer coating, *ACS Appl. Mater. Interfaces*, 6 (4), 2546–2552.
- [50] Liu, X., Li, H., Li, D., Ishida, M., and Zhou, H., 2013, PEDOT modified LiNi<sub>1/3</sub>Co<sub>1/3</sub>Mn<sub>1/3</sub>O<sub>2</sub> with enhanced electrochemical performance for lithium ion batteries, *J. Power Sources*, 243, 374–380.
- [51] Wang, Z., Sun, Y., Chen, L., and Huang, X., 2004, Electrochemical characterization of positive electrode material LiNi<sub>1/3</sub>Co<sub>1/3</sub>Mn<sub>1/3</sub>O<sub>2</sub> and compatibility with electrolyte for lithium-ion batteries, *J. Electrochem. Soc.*, 151 (6), A914–A921.
- [52] Tang, Z., Wang, J., Chen, Q., He, W., Shen, C., Mao, X.X., and Zhang, J., 2007, A novel PEO-based composite polymer electrolyte with absorptive glass mat for Li-ion batteries, *Electrochim. Acta*, 52 (24), 6638–6643.
- [53] Cheng, J.H., Pan, C.J., Lee, J.F., Chen, J.M., Guignard, M., Delmas, C., Carlier, D., and Hwang, B.J., 2014, Simultaneous reduction of Co<sup>3+</sup> and Mn<sup>4+</sup> in P2-Na<sub>2/3</sub>Co<sub>2/3</sub>Mn<sub>1/3</sub>O<sub>2</sub> as evidenced by X-ray absorption spectroscopy during electrochemical sodium intercalation, *Chem. Mater.*, 26 (2), 1219–1225.
- [54] Funabiki, A., Inaba, M., and Ogumi, Z., 1997, A.c. impedance analysis of electrochemical lithium intercalation into highly oriented pyrolytic graphite, *J. Power Sources*, 68 (2), 227–231.
- [55] Levi, M.D., Salitra, G., Markovsky, B., Teller, H., Aurbach, D., Heider, U., and Heider, L., 1999, Solid-state electrochemical kinetics of Li-ion intercalation into Li<sub>1-x</sub>CoO<sub>2</sub>: Simultaneous application of electroanalytical techniques SSCV,

- PITT, and EIS, *J. Electrochem. Soc.*, 146 (4), 1279–1289.
- [56] Lu, Y., Zhang, S., Li, Y., Xue, L., Xu, G., and Zhang, X., 2014, Preparation and characterization of carbon-coated NaVPO<sub>4</sub>F as cathode material for rechargeable sodium-ion batteries, *J. Power Sources*, 247, 770–777.
- [57] Shen, W., Wang, C., Liu, H., and Yang, W., 2013, Towards highly stable storage of sodium ions: A Porous Na<sub>3</sub>V<sub>2</sub>(PO<sub>4</sub>)<sub>3</sub>/C cathode material for sodium-ion batteries, *Chem. Eur. J.*, 19 (43), 14712–14718.